Autophagy activators rescue and alleviate pathogenesis of a mouse model with proteinopathies of the TAR DNA-binding protein 43

I-Fang Wang[a,b,c], Bo-Shen Guo[b], Yu-Chih Liu[d], Cheng-Chun Wu[d], Chun-Hung Yang[b], Kuen-Jer Tsai[c,d,1], and Che-Kun James Shen[a,b,1]

[a]Institute of Life Science, National Defense Medical Center, Taipei, Taiwan 11490; [b]Institute of Molecular Biology, Academia Sinica, Taipei, Taiwan 11529; and [c]Institute of Clinical Medicine and [d]Institute of Basic Medical Science, National Cheng Kung University, Tainan, Taiwan 70457

TDP-43 is a multifunctional DNA/RNA-binding protein that has been identified as the major component of the cytoplasmic ubiquitin (+) inclusions (UBIs) in diseased cells of frontotemporal lobar dementia (FTLD-U) and amyotrophic lateral sclerosis (ALS). Unfortunately, effective drugs for these neurodegenerative diseases are yet to be developed. We have tested the therapeutic potential of rapamycin, an inhibitor of the mammalian target of rapamycin (mTOR) and three other autophagy activators (spermidine, carbamazepine, and tamoxifen) in a FTLD-U mouse model with TDP-43 proteinopathies. Rapamycin treatment has been reported to be beneficial in some animal models of neurodegenerative diseases but not others. Furthermore, the effects of rapamycin treatment in FTLD-U have not been investigated. We show that rapamycin treatment effectively rescues the learning/memory impairment of these mice at 3 mo of age, and it significantly slows down the age-dependent loss of their motor function. These behavioral improvements upon rapamycin treatment are accompanied by a decreased level of caspase-3 and a reduction of neuron loss in the forebrain of FTLD-U mice. Furthermore, the number of cells with cytosolic TDP-43 (+) inclusions and the amounts of full-length TDP-43 as well as its cleavage products (35 kDa and 25 kDa) in the urea-soluble fraction of the cellular extract are significantly decreased upon rapamycin treatment. These changes in TDP-43 metabolism are accompanied by rapamycin-induced decreases in mTOR-regulated phospho-p70 S6 kinase (P-p70) and the p62 protein, as well as increases in the autophagic marker LC3. Finally, rapamycin as well as spermidine, carbamazepine, and tamoxifen could also rescue the motor dysfunction of 7-mo-old FTLD-U mice. These data suggest that autophagy activation is a potentially useful route for the therapy of neurodegenerative diseases with TDP-43 proteinopathies.

protein aggregation | neuronal apoptosis

TDP-43 is a 43-kDa, ubiquitously expressed protein, well conserved among eukaryotes (1). This DNA/RNA-binding factor is predominantly located in the nucleus as a dimer (2), and it has been implicated in multiple cellular functions, e.g., transcriptional repression, splicing, and translation (3–6). TDP-43 has also been identified as the pathological signature protein of a range of neurodegenerative diseases (7). The pathological samples of these diseases, which have been termed TDP-43 proteinopathies, are characterized by cytoplasmic and, to a much lesser extent, nuclear TDP-43-positive (+) and ubiquitinated inclusions (UBIs) containing full-length TDP-43, polyubiquinated TDP-43, phosphorylated TDP-43, as well as 35- and 25-kDa carboxy1 fragments of TDP-43 (for reviews, see refs. 7–11). Of the two major categories of TDP-43 proteinopathies are frontotemporal lobar degeneration with ubiquitin (+) inclusions (FTLD-U) and amyotrophic lateral sclerosis (ALS). It has been estimated that ~50% of FTLD-U and 80–90% of ALS, which has an incidence rate between 1.5 and 2.5 per 100,000 (12), are signified by TDP-43 (+) UBIs (7). Furthermore, numerous experimental data have suggested that misregulation of the metabolism of TDP-43, including

the formation of TDP-43 (+) UBIs, plays a causative role in the pathogenesis (for reviews, see refs. 4, 7, 13). Thus, it would be logical to identify the potential drugs of FTLD-U and ALS with TDP-43 proteinopathies, for which there is no effective drug therapy yet, by targeting either TDP-43 or TDP-43 (+) inclusions.

The molecular machinery of autophagy participates in the removal of long-lived proteins and dysfunctional organelles by inducing the formation of autophagosomes and their fusion with lysosomes to form the autolysosomes (for reviews see refs. 14–16). Autophagy is negatively regulated by the mammalian target of rapamycin (mTOR) (17). Interestingly, whereas TDP-43 is a substrate of the proteasome as well as autophagy (18, 19), it is also required for maintenance of the autophagy by stabilization of the ATG7 mRNA (20). Recent studies have revealed that rapamycin could provide a neuroprotective effect in several neurodegenerative disease models, including Huntington disease (21), Alzheimer's disease (22, 23), and Parkinson disease (24). Besides its antiaging and antiinflammation effects, rapamycin seems to accelerate the removal of aggregation-prone proteins by autophagy induction (25). However, failures of rapamycin as a therapeutic drug have also been reported. For instance, instead of a decrease in pathological features, treatment with rapamycin increases the cytotoxicity of amyloid-β42 and it shortens the life span, as observed in other Alzheimer's disease animal models (26, 27). Aggravation of neuron deaths in one ALS model study (28) has also been observed, indicating that the different pathological mechanisms very likely have drastically different responses to rapamycin treatment.

To test whether rapamycin could be used as an effective therapeutic drug for neurodegenerative diseases with TDP-43 proteinopathies, we used a FTLD-U mouse model for medical experimentation. These FTLD-U mice carried a TDP-43 transgene specifically overexpressed in the forebrain under the control of the Ca^{2+}/calmodulin-dependent kinase II (CamKII) promoter. At 2 mo of age, they started to exhibit cognition impairment, and motor dysfunction became apparent at the age of 6 mo (29). Various molecular and cellular abnormalities also developed along with behavioral phenotypes, which included down-regulation of several markers of neuronal plasticity, neuronal loss, hippocampal atrophy, etc. Most significantly, TDP-43 proteinopathies became obvious at 6 mo of age, with the appearance of polyubiquinated TDP-43 and the 35-kDa and

25-kDa fragments in the urea-soluble fractions of the cellular extracts of the forebrain.

In the following, we show that rapamycin as well as three other autophagy activators could rescue and/or slow down the pathogenesis of the FTLD-U mice described above, thus pointing to a therapeutic route for treatment of FTLD-U and possibly diseases with TDP-43 proteinopathies in general.

Results

Rapamycin Rescued the Impairment of Learning/Memory Capabilities and Alleviated the Progressive Loss of Motor Function in FTLD-U Mice.

For drug treatment, FTLD-U mice were injected with rapamycin (10 mg/kg) or vehicle three times a week for a period of 4 mo from the age of 2 mo. During the treatment, the mice were subjected to the Morris water maze test (30) at the age of 3 mo and to the rotarod test at the age of 6 mo (Fig. 1A). As shown in Fig. 1B, the escape latency of TDP-43 transgenic (Tg) mice treated with rapamycin for 1 mo was significantly shorter than of the vehicle-treated
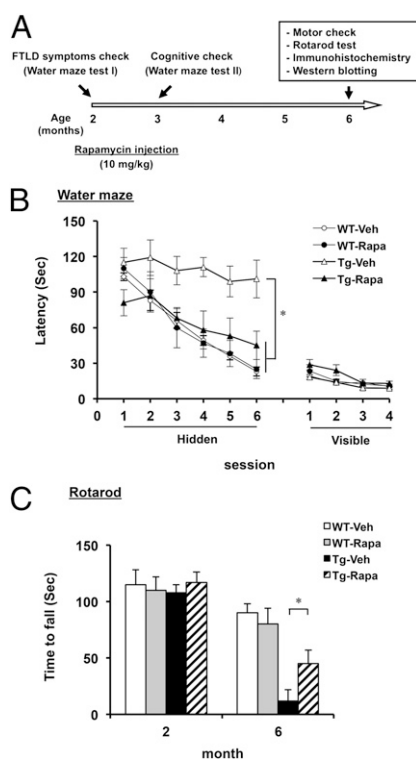

Fig. 1. Phenotype characterizations of rapamycin-treated FTLD-U mice. (A) Flowchart of rapamycin treatment of mice. WT and TDP-43 Tg mice were treated with vehicle or rapamycin as described in Materials and Methods. Treatment continued from the age of 2 mo to the age of 6 mo. Water maze tests (I and II) were carried out at the ages of 2 mo and 3 mo, respectively, and the rotarod test was carried out at the age of 6 mo. (B) Water maze performances of 3-mo-old WT and TDP-43 Tg mice after treatment with rapamycin or vehicle for 1 mo. Note the rescued performance of the Tg mice in the hidden platform tasks (Left) after treatment with rapamycin (Tg-Rapa) in comparison with the ones treated with vehicle (Tg-Veh). Visible platform tasks (Right) of the mice were examined after the hidden platform tasks. Mixed-design ANOVA on the escape latencies across the day indicates the significance of comparisons between the sessions (within-subjects factor, $F(3.36, 53.74) = 442.62$; $P < 0.0001$) and the groups (between-subjects factor, $(F(3,16) = 249.4$; $P < 0.0001$). Results in B represent the mean ± SEM of three independent experiments ($n = 10$ male mice per group). (C) Rotarod performances of 6-mo-old WT and TDP-43 Tg mice after treatment with rapamycin or vehicle for 4 mo. Note the better performance of the Tg-Rapa mice than the Tg-Veh mice. Results in C represent the mean ± SEM of three independent experiments ($n = 10$ male mice per group). *$P < 0.05$.

Tg mice. At the same time, the visible platform tasks showed no differences in swim speed, movement, and visual ability, respectively, among the mice tested (Fig. 1B).

The TDP-43 Tg mice were severely impaired in motor coordination, balance, and grip strength at the age of 6 mo (29). However, the rotarod performance of the rapamycin-treated TDP-43 Tg mice at the age of 6 mo was significantly better in comparison with the vehicle-treated Tg mice (Fig. 1C). To examine whether rapamycin treatment ameliorated the motor function of the TDP-43 Tg mice at the age of 6 mo by reducing motor neuronal loss, Nissl staining of the lumbar spinal cord section was performed. However, numbers of motor neurons were similar between the vehicle- and rapamycin-treated Tg mice (Fig. S1). Overall, the data in Fig. 1 indicated that rapamycin injection could rescue the impairment of learning/memory capabilities of the TDP-43 Tg mice at the age of 3 mo and it also significantly slowed down the age-dependent progressive loss of their motor function.

Rapamycin Reduced the Neuronal Apoptosis via Modulation of the Caspase-3–Dependent Pathway in FTLD-U Mouse Brains.

The TDP-43 Tg mice exhibited a caspase-3–dependent neuronal apoptosis in the hippocampus and cortex at the age of 6 mo (29). To determine whether the improvement of the spatial learning/memory capability of TDP-43 Tg mice upon rapamycin treatment was due to, at least in part, the reduction in neuronal apoptosis, we examined the expression levels of both the procaspase-3 and active caspase-3 by Western blot analysis (Fig. 2A). The result showed that, as previously described (29), amounts of both pro- and active forms of caspase-3 were increased in the hippocampus and cortex of TDP-43 Tg mice compared with wild-type (WT) mice (compare lanes 1 and 3, Fig. 2A). After rapamycin treatment, levels of both pro- and active forms of caspase-3 in the cortex and hippocampus of TDP-43 Tg mice (compare lanes 3 and 4, Fig. 2A), but not WT mice (compare lanes 1 and 2, Fig. 2A), were significantly decreased. The decrease of active caspase-3 in the rapamycin-treated TDP-43 Tg mouse brains was confirmed by caspase-3 activity assay and by immunostaining analysis of the brain sections (Fig. 2 B and C). Significantly, the decrease of caspase-3 levels after rapamycin treatment was coupled with an increase in neurons as shown by anti-NeuN staining (Fig. 2D). In addition, we performed TUNEL assay and anti-GFAP staining to access possible neuroprotective effects of rapamycin. The results showed that not only could rapamycin treatment reduce the number of apoptotic cells, but it also decreased astroglial activation/gliosis-induced neurodegeneration in FTLD-U mouse brains (Fig. S2 A and B). The data of Fig. 2 together with Fig. S2 indicated that rapamycin treatment could reduce neuronal apoptosis in FTLD-U mice via modulation of the caspase-3–dependent pathway.

Rapamycin Inhibited Formation of TDP-43 (+) Inclusions and Reduced Amounts of Abnormally Processed TDP-43 Species in FTLD-U Mouse Brains.

We also examined whether rapamycin treatment had any effect on mismetabolism of TDP-43 in the forebrain of FTLD-U mice. As reported previously (29), both cytosolic TDP-43 (+) UBIs and relatively insoluble forms of TDP-43, including polyubiquitinated TDP-43 and 35-kDa/25-kDa TDP-43 fragments, accumulated in the forebrains of 6-mo-old FTLD-U mice. As shown first by Western blotting analysis, rapamycin treatment did not reduce the amounts of full-length TDP-43 and 35-kDa/25-kDa fragments in the soluble (RIPA) fraction of total extracts from the cortex and hippocampus of 6-mo-old FTLD-U mice (Fig. 3A). On the other hand, expression levels of full-length TDP-43, polyubiquitinated TDP-43 (***), and the 35-kDa fragment, the latter two of which were mainly detectable in the urea-soluble fraction of the forebrain extract, were all down-regulated after 4 mo of rapamycin treatment (Fig. 3B). These data
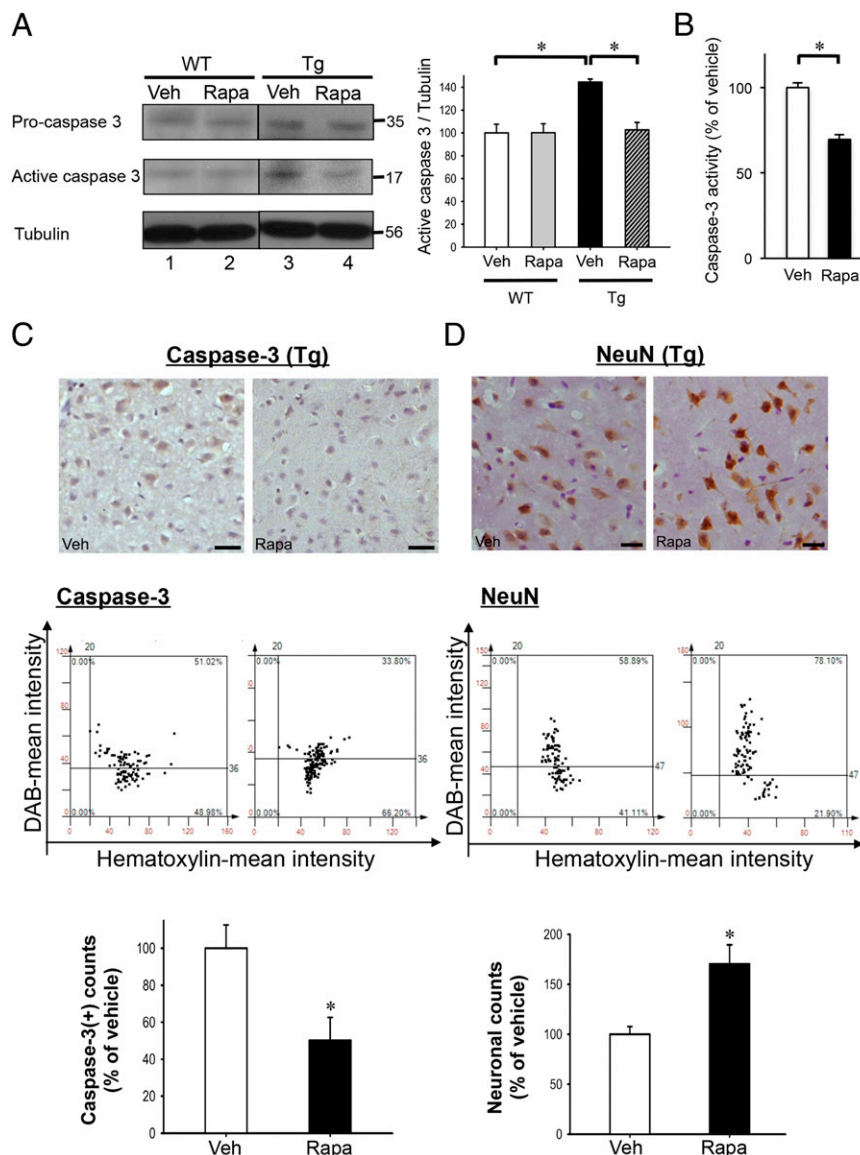
Fig. 2. Rapamycin effects on caspase-3 expression and neuronal survival in FTLD-U mouse brains. (*A*) Western blotting analysis of the levels of pro- and active forms of caspase-3 in the extracts of isolated cortex and hippocampus from 6-mo-old WT and TDP-43 Tg mice treated with rapamycin or vehicle. Blotting patterns are shown on the *Left* and the statistical analysis is shown on the *Right*. Results are representative of the mean ± SEM of three independent experiments (*n* = 5 mice per group). *$P < 0.05$. (*B*) Measurement of the caspase-3 activities in the extracts from the cortex and hippocampus of TDP-43 Tg mice treated with rapamycin (Rapa)- or vehicle (Veh) by fluorimetric assay. Histogram represents caspase-3 activities (mean ± SEM) of three independent experiments (*n* = 3 mice per group). *$P < 0.05$. (*C*) Immunohistostaining analysis of active caspase-3 (*Top* two panels) in the cortex of 6-mo-old TDP-43 Tg mouse brains treated with rapamycin (Rapa) or vehicle (Veh) for 4 mo. Quantitative analysis by tissue cytometry using TissueQuest software is shown in the *Middle* and the *Bottom* histograms. (*D*) Immunohistostaining of NeuN(+) cells in the cortex of 6-mo-old TDP-43 Tg mice treated with rapamycin (Rapa) or vehicle (Veh) for 4 mo (*Top* two panels). Quantitative analysis is shown in the *Middle* two panels and the *Bottom* histogram. Results in both *C* and *D* represent the mean ± SEM of three independent experiments (*n* = 5 mice per group). (Bars, 25 μm.) *$P < 0.05$.

suggested that rapamycin treatment might also inhibit the process of aggregate formation of mismetabolized TDP-43 species. Indeed, as shown by immunohistochemistry and hematoxylin staining of the brain sections, the number of forebrain cells with cytosolic TDP-43 (+) inclusions and TDP-43 depleted nuclei in 6-mo-old FTLD-U mice was greatly reduced after treatment with rapamycin (Fig. 3*C*). In contrast to Tg mice (Fig. 3*B*), the 35-kDa/25-kDa fragments were barely detectable in the urea-soluble fraction of the forebrain extract from the WT mice (Fig. S3*A*). Furthermore, the forebrain cells of the WT mice contained no TDP-43 (+) inclusion without or with rapamycin treatment (Fig. S3*B*). Overall, the data of Fig. 3 indicated that rapamycin treatment inhibited the formation of TDP-43 (+) inclusions in the

diseased cells of the FTLD-U mouse brains, likely due to its capacity for enhancing autophagic clearance, which would degrade the abnormally generated TDP-43 species before their aggregation in the cytosol.

Therapeutic Effects of Rapamycin Were Associated with Activation of mTOR-Regulated Autophagy in FTLD-U Mouse Brains. To investigate whether the abolishment of the TDP-43 (+) inclusions in the forebrains of FTLD-U mice by rapamycin treatment was coupled with the mTOR-regulated autophagy process, we examined the levels of several autophagic and mTOR activity markers by immunofluorescence staining and/or Western blotting. As shown in Fig. 4*A*, the autophagosome marker LC3-positive puncta, which
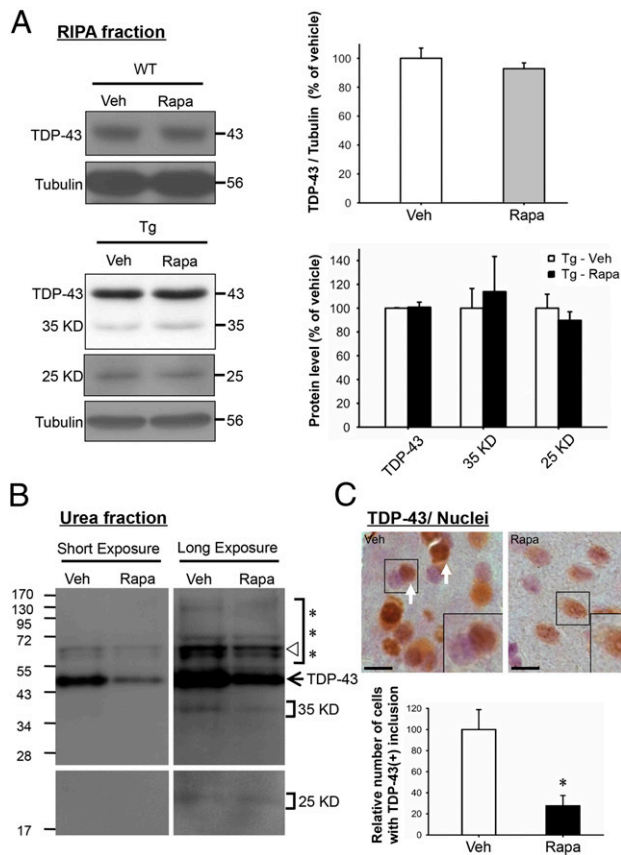
Fig. 3. Rapamycin effects on the solubility and subcellular distribution of TDP-43 in FTLD-U mouse brains. (*A*) Western blot analysis of TDP-43 in the soluble/ RIPA fractions of extracts from the cortex and hippocampus regions of 6-mo-old WT (*Upper* set of panels and histogram) and TDP-43 Tg mice (*Lower* set of panels and histogram) treated with rapamycin or vehicle. The RIPA fractions of the extracts were prepared as described in *Materials and Methods* and analyzed by Western blotting. Note that rapamycin and vehicle treatments resulted in similar levels of the different TDP-43 species in either the WT or the Tg mouse samples. Amounts of the 35-kDa and 25-kDa TDP-43 fragments in the WT extract were too low to be analyzed. (*B*) Western blot analysis of TDP-43 in the urea-soluble fractions of brain extracts. The arrow points to the unmodified form of TDP-43 on the gel. The triangle is an anti–TDP-43 hybridizing band of unknown origin. ***, represents the gel region containing high molecular weight, polyubiquitinated TDP-43 species. Result is representative of three independent experiments. (*C*) Immunohistochemical staining of TDP-43 and nuclei of brain sections from TDP-43 Tg mice treated with rapamycin or vehicle. Sections were immunohistochemically stained for detection of TDP-43 (brown) and nuclei (blue) as described in *Materials and Methods*. TDP-43 (+) inclusions are indicated by white arrows. One cell each from the two images are further magnified in the *Lower Right* corners for better visualization. (Bars, 10 μm.) Quantitative analysis of the relative numbers of TDP-43 (+) inclusions is shown in the histogram below the photo panels. Results in *A* and *C* represent the mean ± SEM of three independent experiments (*n* = 5 mice per group). *$P < 0.05$.

represented the presence of autolysosomes, were significantly elevated in the cortex region of rapamycin-treated FTLD-U mice compared with vehicle-treated ones (Fig. 4*A*). During autophagosome formation, LC3-I is processed to LC3-II by lipidation. Thus, the level of LC3-II would increase during synthesis of the autophagosome (15). Consistent with the observation in Fig. 4*A*, we found that the ratios of LC3-II/LC3-I in the cortex and hippocampus regions of rapamycin-treated FTLD-U as well as WT mice were significantly increased compared with vehicle-treated mice (Fig. 4 *B a* and *B b*), indicating that rapamycin enhanced autophagosome formation and also triggered the latter steps of

autolysosome formation during the autophagy process. Interestingly, the level of p62/SQSTM1, an autophagic flux marker down-regulated along the autophagy pathway (31), in the cortex and hippocampus of vehicle-treated FTLD-U mouse brain was higher than that of the vehicle-treated WT mouse brain, indicating an incomplete autophagy in the mouse brain upon overexpression of TDP-43 (Fig. 4 *B a* and *B c*). Upon rapamycin treatment, however, the levels of p62 in the cortex and hippocampus of both FTLD-U and WT mice were reduced (Fig. 4 *B a* and *B c*), suggesting the enhancement of autophagy in the WT mouse brain and rescue of autophagy in the FTLD-U mouse brain, respectively. The above observations were indeed the results of inhibition of the mTOR signaling pathway by rapamycin, as reflected by the reductions in the levels of phospho-p70
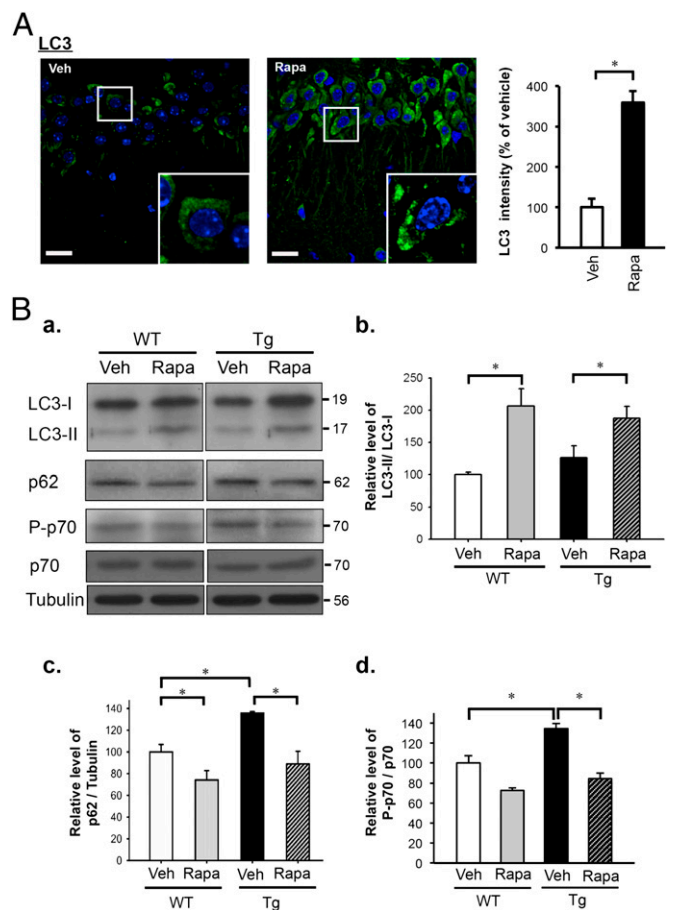

Fig. 4. Effects of rapamycin treatment on autophagy in the forebrains of WT and TDP-43 Tg mice. (*A*, *Left*) representative immunofluorescence images of the hippocampus of TDP-43 Tg mice treated with rapamycin/vehicle and costained with anti-LC3 (green)/DAPI (blue). Note the increase of the LC3 puncta in the rapamycin-treated Tg mouse sample in comparison with the vehicle-treated one. (Bars, 10 μm.) (*Right*) Histogram of quantification of LC3 immunofluorescence. Result is representative of three independent experiments (*n* = 5 sections per group). *$P < 0.05$. (*B*) Western blot analysis of expression levels of LC3, p62, P-p70, and p70 S6 kinase. Levels of proteins and tubulin control in the extracts of the isolated cortex and hippocampus from WT and TDP-43 Tg mice with or without rapamycin treatment were measured by Western blotting. (*a*) Blot patterns. Comparisons among WT and Tg mice treated with rapamycin (Rapa) or vehicle (Veh) are shown in the histograms for LC3-II normalized with LC3-I (*b*), p62 normalized with tubulin (*c*), and P-p70 normalized with p70 (*d*), respectively. For all three histograms, the protein levels are first normalized and then compared with WT (Veh) samples. Results represent the mean ± SEM of three independent experiments (*n* = 5 mice per group). *$P < 0.05$.

S6 kinase (P-p70) in the cortex and hippocampus regions of the brains of rapamycin-treated FTLD-U as well as WT mice in comparison with vehicle-treated mice (Fig. 4 *B a* and *B d*).

Autophagy Activation in General Rescued Motor Dysfunction Through Reduction of Cytosolic TDP-43 (+) Inclusions and Enhancement of Neuronal Survival. We have also tested the effects of rapamycin and three other chemical drugs, spermidine, carbamazepine, and tamoxifen, in the rescue of motor dysfunction of FTLD-U mice. Of these other three chemicals, tamoxifen was also an inhibitor of m-TOR, whereas spermidine and carbamazepine activated autophagy via the mTOR-independent pathway. As shown in Fig. 5*A*, treatment of 6-mo-old FTLD-U mice with any of the four chemicals for 1 mo significantly improved the performance in rotarod tests. Significantly, the improvement of motor coordination of the mice by treatment with these four drugs was associated with neuronal protection, as reflected by the increase in neuron numbers (Fig. 5*B*) and by reduction of the number of forebrain cells containing TDP-43 (+) inclusions (Fig. 5*C*) in drug-treated mice. Finally, the rescues and neuron protection of the 7-mo-old FTLD-U mice by the four drugs were indeed accompanied by autophagy activation, as indicated by the increase of LC3-II/LC3-I ratio (Fig. 5 *D a* and *D b*) and reduction of the level of p62/SQSTM1 (Fig. 5 *D a* and *D c*). The data of Fig. 5 indicated that autophagy activation through mTOR-dependent as well as mTOR-independent pathways could also rescue motor dysfunction of FTLD-U mice.

Discussion

The above study has shown that mTOR inhibition by rapamycin could recover the learning/memory capability and ameliorate motor neuron function of TDP-43 Tg mice with pathological phenotypes of FTLD-U. Furthermore, the phenotypic recoveries are accompanied by the clearance of TDP-43 (+) UBIs in FTLD-U mouse brains through autophagy. This therapeutic effect of rapamycin can also be observed in other models of neurodegenerative diseases, such as the improvement of neurodegeneration and motor dysfunction in fly and mouse models of Huntington disease (21), reducing of tau-mediated toxicity in transgenic flies (25), and the rescue of learning/memory deficits in two different Alzheimer's disease mouse models (22, 23). In parallel, it has been found that rapamycin, through the enhancement of autophagy, could help the clearance of aggregation-prone proteins, including the mutant huntingtin protein (21), α-synuclein (24, 32), β-amyloid (23), and the pathological prion protein (33). In great contrast, however, it has been found that rapamycin treatment could not rescue the phenotype of an ALS mouse model with transgenic overexpression of the mutant SOD1 G93A protein (28). Indeed, induction of the autophagosome formation without parallel enhancement of the autophagic flux may result in further accumulation of aggregated protein and trigger more severe cytotoxicity. Such negative outcomes of the use of rapamycin as a therapeutic agent have also been found in other Alzheimer's disease animal models (26, 27, 34). Thus, autophagy activation by rapamycin and other autophagy-enhancing drugs may not be generally applicable for the treatment of different neurodegenerative diseases, and case-by-case studies should be carried out.

In the case of our FTLD-U mice, rapamycin treatment reduces the amounts of insoluble TDP-43 species (Fig. 3*B*) as well as the formation of TDP-43 (+) inclusions (Fig. 3*C*) in the forebrain region of the TDP-43 Tg mice. This was accompanied by a recovery of autophagy as indicated by the analysis of different autophagy markers (Fig. 4). However, the levels of the soluble nonaggregate forms of the different TDP-43 species were not affected by rapamycin treatment. Our data are consistent with previous findings in cultured cells showing that neither autophagy inhibitor 3-MA nor autophagy enhancer rapamycin could alter the endogenous level of the TDP-43 protein (35). Furthermore, the
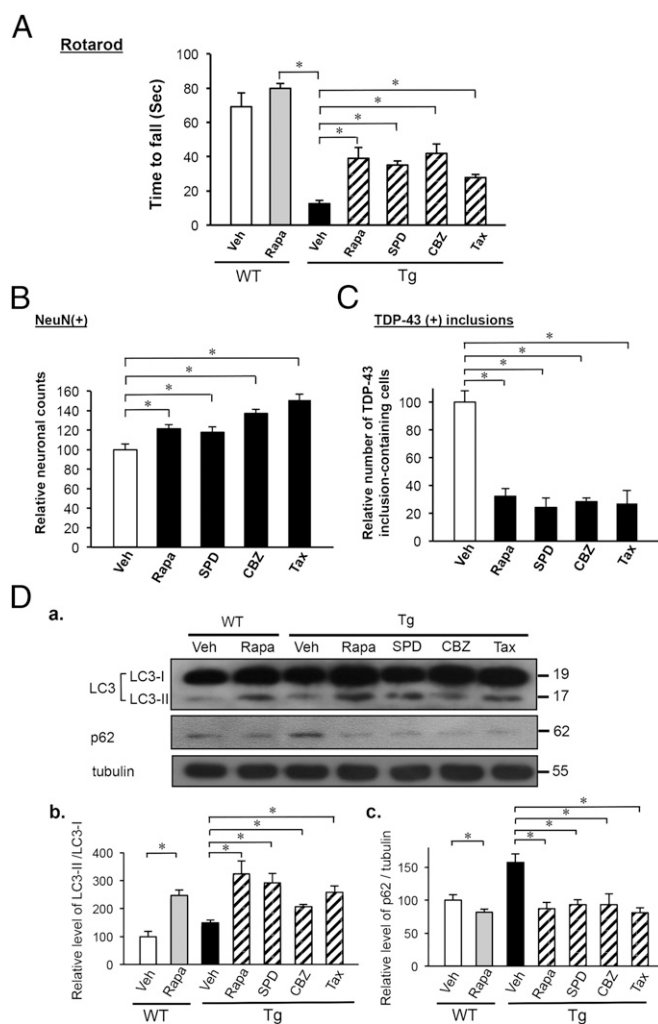

Fig. 5. Effects of autophagy activation in the rescue of motor dysfunction of 7-mo-old CamKII–TDP-43 Tg mice. (*A*) Rotarod tests of 7-mo-old CamKII–TDP-43 Tg mice after treatment with rapamycin, spermidine, carbamazepine, tamoxifen, or vehicle for 1 mo, as described in *Materials and Methods*. As the control, FVB/NJNarl-WT mice treated with rapamycin or vehicle at the same age were also tested. Note the improvement of the rotarod performance of the TDP-43 Tg mice upon treatment with each of the four chemicals. Data represent the mean ± SEM of three independent experiments (*n* = 10 mice per group). *P < 0.05. (*B*) Quantitative comparison of the relative abundance of NeuN(+) cells in the brain sections of 7-mo-old TDP-43 Tg mice treated with rapamycin, spermidine, carbamazepine, tamoxifen, or vehicle for 1 mo. The number of NeuN(+) cells of the vehicle samples is taken as 100 (*n* = 5 mice per group). *P < 0.05. (*C*) Histograms showing quantitative analysis of the relative numbers of TDP-43 (+) inclusion-containing cells in the cortex sections from 7=mo-old TDP-43 Tg mice that were treated with rapamycin, spermidine, carbamazepine, tamoxifen, or vehicle for 1 mo. The number of vehicle samples is taken as 100. Results in *B* and *C* represent the mean ± SEM of three independent experiments (*n* = 5 mice per group). *P < 0.05. (*D*) Western blot analysis of expression levels of LC3-I, LC3-II, and p62. Levels of proteins in the extracts of isolated cortex and hippocampus from 7-mo-old WT and TDP-43 Tg mice with or without drug treatment were analyzed and compared. (*a*) Representative Western blot. (*b*) Histogram comparing the ratios of LC3-II/LC3-I in different samples. (*c*) Histogram comparing the ratios of p62/tubulin in different samples. In both *b* and *c*, the ratios of WT (Veh) samples were taken as 100. The altered level of LC3-II and the accumulation of p62 in Tg mice relative to WT mice indicate the impairment of autophagy, which has also been observed in a SOD-1 (G93A) Tg mouse model (28). Results represent the mean ± SEM of three independent experiments (*n* = 5 mice per group). *P < 0.05.

full-length TDP-43 and its C-terminal fragments in the insoluble (urea soluble) fraction accumulated under autophagy inhibition by 3-MA, whereas no significant changes of amounts of TDP-43

species in the RIPA soluble fraction could be detected (19). Thus, our data provide unique in vivo evidence that rapamycin-induced autophagy could play an active role in the clearance of TDP-43 aggregates and in the reduction of inclusion formation, possibly in part through binding of the inclusions with p62/SQSTM1 (36) and subsequent autophagic degradation (37). Finally, the significant improvements in motor behaviors of the FTLD-U mice and the increase in neuronal survivability accompanied by reduction of cytosolic TDP-43 (+) inclusions upon treatment with three other autophagy activators as well as rapamycin (Fig. 5) indicate that autophagy induction is likely beneficial in disease mitigation of TDP-43 proteinopathies. It should be noted that the effect of rescue of motor function of the mice by treatment with any given autophagy enhancer at the age of 6 mo likely would not be as great as treatment starting at an early pathological stage, e.g., 2 mo of age (compare Figs. 5*A* and 1*C*), because the neuronal degeneration is more extensive in the brains of 6-mo-old TDP-43 Tg mice (29). The similar extents in reduction of the number of forebrain cells with TDP-43 (+) inclusions in FTLD-U mice upon early and late treatments, respectively, with the drugs (compare Figs. 3*C* and 5*C*) suggest that the autophagy activators could prevent the formation of, as well as remove, the cytosolic TDP-43 (+) inclusions.

In summary, we have demonstrated that autophagy activation is an effective route for therapy of TDP-43 Tg mice with FTLD-U phenotypes. In particular, the elevation of the LC3-I/LC3-II and

reduction of p62 upon rapamycin treatment indicate that the cells in the forebrain of the mice, despite overexpression of TDP-43 and formation of the TDP-43 (+) inclusions, still maintain an autophagy system, albeit impaired, that is responsive to and reusable by pharmacological stimuli. The therapeutic effects of spermidine, carbamazepine, and tamoxifen indeed support this conclusion. Thus, this study has set the basis for future therapy of neurodegenerative diseases with TDP-43 proteinopathies by pharmacologically targeting autophagy.

Materials and Methods

Rapamycin powder (Sirolimus; LC Laboratories) was dissolved in ethanol and stored at −20 °C in aliquots of the concentration of 50 mg/mL. The working solution was prepared freshly before use with a final concentration of 1 mg/mL rapamycin in 2% (vol/vol) ethanol. For the behavioral tests, the WT and TDP-43 Tg (+/+) male mice of 2 mo of age were injected intraperitoneally with rapamycin (10 mg/kg) three times a week for a period of 4 mo. The control animals were injected with PBS (vehicle) in parallel. For more information about drug treatment and additional experimental details, please see *SI Materials and Methods*.

1. Wang HY, Wang IF, Bose J, Shen CK (2004) Structural diversity and functional implications of the eukaryotic TDP gene family. *Genomics* 83:130–139.
2. Kuo PH, Doudeva LG, Wang YT, Shen CK, Yuan HS (2009) Structural insights into TDP-43 in nucleic-acid binding and domain interactions. *Nucleic Acids Res* 37:1799–1808.
3. Buratti E, Baralle FE (2008) Multiple roles of TDP-43 in gene expression, splicing regulation, and human disease. *Front Biosci* 13:867–878.
4. Wang IF, Wu LS, Shen CK (2008) TDP-43: An emerging new player in neurodegenerative diseases. *Trends Mol Med* 14:479–485.
5. Lagier-Tourenne C, Polymenidou M, Cleveland DW (2010) TDP-43 and FUS/TLS: Emerging roles in RNA processing and neurodegeneration. *Hum Mol Genet* 19(R1): R46–R64.
6. Polymenidou M, et al. (2011) Long pre-mRNA depletion and RNA missplicing contribute to neuronal vulnerability from loss of TDP-43. *Nat Neurosci* 14:459–468.
7. Chen-Plotkin AS, Lee VM, Trojanowski JQ (2010) TAR DNA-binding protein 43 in neurodegenerative disease. *Nat Rev Neurol* 6:211–220.
8. Arai T, et al. (2006) TDP-43 is a component of ubiquitin-positive tau-negative inclusions in frontotemporal lobar degeneration and amyotrophic lateral sclerosis. *Biochem Biophys Res Commun* 351:602–611.
9. Neumann M, et al. (2006) Ubiquitinated TDP-43 in frontotemporal lobar degeneration and amyotrophic lateral sclerosis. *Science* 314:130–133.
10. Neumann M, et al. (2009) Phosphorylation of S409/410 of TDP-43 is a consistent feature in all sporadic and familial forms of TDP-43 proteinopathies. *Acta Neuropathol* 117:137–149.
11. Da Cruz S, Cleveland DW (2011) Understanding the role of TDP-43 and FUS/TLS in ALS and beyond. *Curr Opin Neurobiol* 21:904–919.
12. Logroscino G, et al.; EURALS (2008) Descriptive epidemiology of amyotrophic lateral sclerosis: New evidence and unsolved issues. *J Neurol Neurosurg Psychiatry* 79:6–11.
13. Kwong LK, Neumann M, Sampathu DM, Lee VM, Trojanowski JQ (2007) TDP-43 proteinopathy: The neuropathology underlying major forms of sporadic and familial frontotemporal lobar degeneration and motor neuron disease. *Acta Neuropathol* 114:63–70.
14. Mizushima N, Klionsky DJ (2007) Protein turnover via autophagy: Implications for metabolism. *Annu Rev Nutr* 27:19–40.
15. Kundu M, Thompson CB (2008) Autophagy: Basic principles and relevance to disease. *Annu Rev Pathol* 3:427–455.
16. Weidberg H, Shvets E, Elazar Z (2011) Biogenesis and cargo selectivity of autophagosomes. *Annu Rev Biochem* 80:125–156.
17. Díaz-Troya S, Pérez-Pérez ME, Florencio FJ, Crespo JL (2008) The role of TOR in autophagy regulation from yeast to plants and mammals. *Autophagy* 4:851–865.
18. Kim SH, et al. (2009) Potentiation of amyotrophic lateral sclerosis (ALS)-associated TDP-43 aggregation by the proteasome-targeting factor, ubiquilin 1. *J Biol Chem* 284: 8083–8092.
19. Brady OA, Meng P, Zheng Y, Mao Y, Hu F (2011) Regulation of TDP-43 aggregation by phosphorylation and p62/SQSTM1. *J Neurochem* 116:248–259.
20. Bose JK, Huang CC, Shen CK (2011) Regulation of autophagy by neuropathological protein TDP-43. *J Biol Chem* 286:44441–44448.

21. Ravikumar B, et al. (2004) Inhibition of mTOR induces autophagy and reduces toxicity of polyglutamine expansions in fly and mouse models of Huntington disease. *Nat Genet* 36:585–595.
22. Caccamo A, Majumder S, Richardson A, Strong R, Oddo S (2010) Molecular interplay between mammalian target of rapamycin (mTOR), amyloid-beta, and Tau: Effects on cognitive impairments. *J Biol Chem* 285:13107–13120.
23. Spilman P, et al. (2010) Inhibition of mTOR by rapamycin abolishes cognitive deficits and reduces amyloid-beta levels in a mouse model of Alzheimer's disease. *PLoS ONE* 5:e9979.
24. Crews L, et al. (2010) Selective molecular alterations in the autophagy pathway in patients with Lewy body disease and in models of alpha-synucleinopathy. *PLoS ONE* 5: e9313.
25. Berger Z, et al. (2006) Rapamycin alleviates toxicity of different aggregate-prone proteins. *Hum Mol Genet* 15:433–442.
26. Bové J, Martínez-Vicente M, Vila M (2011) Fighting neurodegeneration with rapamycin: Mechanistic insights. *Nat Rev Neurosci* 12:437–452.
27. Ling DJ, Song HJ, Garza D, Neufeld TP, Salvaterra PM (2009) Abeta42-induced neurodegeneration via an age-dependent autophagic-lysosomal injury in Drosophila. *PLoS ONE* 4:e4201.
28. Zhang X, et al. (2011) Rapamycin treatment augments motor neuron degeneration in SOD1(G93A) mouse model of amyotrophic lateral sclerosis. *Autophagy* 7:412–425.
29. Tsai KJ, et al. (2010) Elevated expression of TDP-43 in the forebrain of mice is sufficient to cause neurological and pathological phenotypes mimicking FTLD-U. *J Exp Med* 207:1661–1673.
30. Tsai KJ, Tsai YC, Shen CK (2007) G-CSF rescues the memory impairment of animal models of Alzheimer's disease. *J Exp Med* 204:1273–1280.
31. Pankiv S, et al. (2007) p62/SQSTM1 binds directly to Atg8/LC3 to facilitate degradation of ubiquitinated protein aggregates by autophagy. *J Biol Chem* 282:24131–24145.
32. Webb JL, Ravikumar B, Atkins J, Skepper JN, Rubinsztein DC (2003) Alpha-Synuclein is degraded by both autophagy and the proteasome. *J Biol Chem* 278:25009–25013.
33. Heiseke A, Aguib Y, Riemer C, Baier M, Schätzl HM (2009) Lithium induces clearance of protease resistant prion protein in prion-infected cells by induction of autophagy. *J Neurochem* 109:25–34.
34. Zhang SQ, et al. (2010) Rapamycin promotes beta-amyloid production via ADAM-10 inhibition. *Biochem Biophys Res Commun* 398:337–341.
35. Caccamo A, et al. (2009) Rapamycin rescues TDP-43 mislocalization and the associated low molecular mass neurofilament instability. *J Biol Chem* 284:27416–27424.
36. Pikkarainen M, Hartikainen P, Alafuzoff I (2008) Neuropathologic features of frontotemporal lobar degeneration with ubiquitin-positive inclusions visualized with ubiquitin-binding protein p62 immunohistochemistry. *J Neuropathol Exp Neurol* 67: 280–298.
37. Bjørkøy G, et al. (2005) p62/SQSTM1 forms protein aggregates degraded by autophagy and has a protective effect on huntingtin-induced cell death. *J Cell Biol* 171: 603–614.

NEUROSCIENCE